11. Measurements were made with the XTM on the 31-pole wiggler beam line (BL-10) at Stanford Synchrotron Radiation Laboratory. A double-crystal monochromator [Si(220) reflections] was used for the selection of energies between 20 and 27 keV. High-resolution radiographic images were taken as the sample rotated in 0.5° increments from 0° to 180°. These images were normalized to the incident beam and reconstructed into 3D images with the use of Fourier-filtered back projection.
12. The mass-absorption coefficient for Nicalon was determined by the use of tabulated data from E. F. Plechaty *et al.*, in *Tables and Graphs of Photon-Interaction Cross Sections* (Lawrence Livermore National Laboratory, Livermore, CA, 1981), vol 6, rev. 3. The composition of Nicalon was considered to be (by weight) 59% Si, 31% C, and 10% O. A density of 2.6 g $cm^{-3}$ was used for Nicalon.
13. T. M. Breunig, M. C. Nichols, J. H. Kinney, paper presented at the 17th Annual Conference on Composites and Advanced Ceramics, Cocoa Beach, FL, 11 to 15 January 1993.
14. We thank A. M. Gokhale for valuable discussions regarding stereology, A. Gardea for sample preparation, W. Massey for electronics engineering support, J. Daniel for artwork, and J. Bruner for editorial assistance. Supported by the U.S. Department of Energy (DOE), Advanced Industrial Concepts Materials Program ED38-02, and performed under the auspices of the U.S. DOE by the Lawrence Livermore National Laboratory under contract W-7405-Eng-48 and by Sandia National Laboratories California under Contract DE-AC04-76DP00789; the Stanford Synchrotron Radiation Laboratory is supported by the U.S. DOE, Chemical Sciences Division.

3 December 1992; accepted 23 February 1993

# The Nitrogenase FeMo-Cofactor and P-Cluster Pair: 2.2 Å Resolution Structures

Michael K. Chan, Jongsun Kim, D. C. Rees*

**Structures recently proposed for the FeMo-cofactor and P-cluster pair of the nitrogenase molybdenum-iron (MoFe)–protein from *Azotobacter vinelandii* have been crystallographically verified at 2.2 angstrom resolution. Significantly, no hexacoordinate sulfur atoms are observed in either type of metal center. Consequently, the six bridged iron atoms in the FeMo-cofactor are trigonally coordinated by nonprotein ligands, although there may be some iron-iron bonding interactions that could provide a fourth coordination interaction for these sites. Two of the cluster sulfurs in the P-cluster pair are very close together (~2.1 angstroms), indicating that they form a disulfide bond. These findings indicate that a cavity exists in the interior of the FeMo-cofactor that could be involved in substrate binding and suggest that redox reactions at the P-cluster pair may be linked to transitions of two cluster-bound sulfurs between disulfide and sulfide oxidation states.**

There has been considerable interest in the determination of the structures of the nitrogenase proteins and associated metal centers to learn how nature catalyzes the conversion of $N_2$ to $NH_3$ (*1*). This question has been particularly tantalizing because nitrogenase can fix nitrogen at room temperature, whereas the best industrial process requires both high temperatures and pressures. Nitrogenase consists of two component proteins, the MoFe-protein and Fe-protein that together contain three distinct types of redox centers: two unusual Fe-S clusters, the FeMo-cofactor and the P-cluster pair, located within the MoFe-protein, and a single $Fe_4S_4$ cluster bound to the Fe-protein. Recently, we proposed structures (designated the "Kim models") for the P-cluster pair and FeMo-cofactor of the nitrogenase MoFe-protein that were based on x-ray diffraction data collected to 2.7 Å resolution (*2*). The P-cluster pair was described as containing two $Fe_4S_4$ cubane clusters coupled by two bridging cysteine (Cys) thiols, whereas the FeMo-cofactor was modeled as a dimer of $MFe_3S_3$ (M = Fe or Mo) partial cubanes linked by three nonprotein ligands. However, alternative models for both centers were subsequently proposed (*3*). These alternate models for both the FeMo-cofactor and the P-cluster pair are topologically similar to one another and are based on two $MFe_3S_3$ (M = Fe or Mo) clusters linked by a common hexacoordinate S.

To definitively characterize the structures of the metal centers, we collected x-ray diffraction data to 2.2 Å resolution from two *Azotobacter vinelandii* MoFe-protein crystals (*2*) with a MAR Research imaging plate detector at the Stanford Synchrotron Radiation Laboratory. The images were processed with the MOSFLM and CCP4 packages (*4*), yielding a final set of 95,078 reflections (90% complete to 2.2 Å resolution, reduced from a total of 258,519 observations with an $R_{merge}$ of 0.136). Refinement of the MoFe-protein model at 2.2 Å resolution with the program X-PLOR (*5*), followed by TNT (*6*), has progressed to $R$ = 0.202, with root-mean-square (rms) deviations from bond distances and angles of 0.020 Å and 2.98°, respectively. Two types of electron density maps were examined to establish the locations of the metal and S positions in the P-cluster pair (Fig. 1) and FeMo-cofactor (Fig. 2). To define the metal positions, $F_o - F_c$ maps were generated with $F_c$ values calculated from a model that was refined without the metal cofactors and their coordinated ligands. The S positions were then established from $F_o - F_c$ maps with the use of $F_c$ values from a refinement that contained the metal positions but with the cluster S atoms omitted

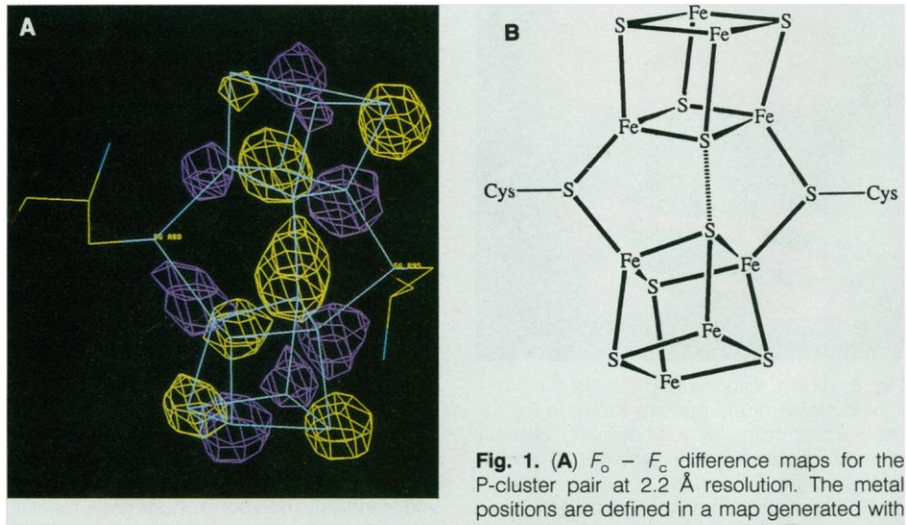


**Fig. 1.** (**A**) $F_o - F_c$ difference maps for the P-cluster pair at 2.2 Å resolution. The metal positions are defined in a map generated with the $F_c$ calculated from a model refined without metal centers and coordinated ligands. The magenta contours represent 12 times the standard deviation of this map. The yellow contours define the sulfur positions in a map with $F_c$ calculated from a model refined without the sulfurs. The yellow contours are 6.7 times the standard deviation of this map. (**B**) Schematic representation of the P-cluster pair in the same orientation as (A).

Division of Chemistry and Chemical Engineering 147-75CH, California Institute of Technology, Pasadena, CA 91125.

*To whom correspondence should be addressed.

from the diffraction term. The highest peaks in each map are completely consistent with the locations of the metal and S sites in the Kim models (Figs. 1 and 2). No hexacoordinate S sites of the type depicted in the alternate models (*3*) are seen in either the FeMo-cofactor or the P-cluster pair.

The 2.2 Å resolution analysis of the P-cluster pair confirms the presence of eight Fe atoms in an arrangement consisting of two $Fe_4S_4$ cubane clusters linked by bridging Cys thiolate groups. With the higher resolution data, we are now able to establish that the two cubane clusters are further joined by a disulfide bridge (bond distance ~2.1 Å) formed between S atoms in each $Fe_4S_4$ cubane cluster. This disulfide bridge is positioned between the two cluster Fe atoms with nontetrahedonal geometry (*2*) and is located on the side of the P-cluster pair closest to the proposed (*7*) binding site for Fe-protein. Unlike other Fe-S clusters containing disulfide bonds, including intermolecular disulfide-bridged $Fe_2S_2$ clusters that have been synthesized previously (*8, 9*), this cluster contains a $(\mu_3\text{-}S)_2$ disulfide. Interestingly, diffraction analyses of older MoFe-protein crystals indicate that the P-cluster pair is depleted in the disulfide-bonded sulfur closest to serine β188 (*10*). This observation suggests that oxygen inactivation of MoFe-protein may be related to the lability of the disulfide-bridged atoms.

The presence of the disulfide bond in the P-cluster pair suggests that this center can act as a two-electron redox group, involving cleavage and reformation of the $\mu_3$-disulfide bridge. In addition to a purely electron transfer function, this disulfide bond may also provide a site for $H_2$ evolution by nitrogenase. Hydrogen production has been suggested to accompany disulfide bond formation between two $Fe_2S_2$ clusters in model systems (*8*). In this case, reaction between two $Fe_2S(SH)$ clusters is thought to generate $H_2$ concomitantly with formation of the disulfide-bridged cluster dimer. It is possible that protonation of the doubly reduced P-cluster pair may generate a similar species that can produce $H_2$ upon disulfide bond formation, and that this mechanism could contribute to the hydrogenase activity of nitrogenase.

The disulfide bridge also suggests a possible mechanism linking protein conformational changes to redox reactions at the P-cluster pair. As the P-cluster pair is at the αβ-subunit interface in the MoFe-protein and because this region of the MoFe-protein appears to interact with the Fe-protein (*7*), conformational alterations induced by nucleotide hydrolysis of the Fe-protein could influence the redox behavior of the P-cluster pair. As the nonbridging ligands coordinating each $Fe_4S_4$ cluster in the P-cluster pair originate from the same subunit, allosteric changes at this interface could lead to an increased separation between the two $Fe_4S_4$ units, facilitating disulfide bond cleavage. Breakage of this disulfide bond would require an internal redox reaction whose net effect would be the oxidation of each $Fe_4S_4$ cluster by one electron, thereby making electron transfer from the Fe-protein to the P-cluster pair thermodynamically more favorable. Dissociation of the MoFe-protein–Fe-protein complex would allow the P-cluster pair disulfide bond to reform, yielding a P-cluster pair containing "super-reduced" electrons. The production and transfer of these electrons to the FeMo-cofactor may be necessary to overcome a critical activation barrier in the reduction of nitrogen to ammonia. This postulated linkage between protein conformation and P-cluster pair oxidation state may help to explain the requirement of magnesium adenosine triphosphate (MgATP) in the nitrogenase reaction.

The 2.2 Å resolution difference map for the FeMo-cofactor (Fig. 2) also confirms the Kim model in that the FeMo-cofactor consists of two $MFe_3S_3$ (M = Mo or Fe) clusters linked by two bridging sulfides and a third ligand, designated Y. Compared with the other two bridging ligands (Fig. 2), Y has ~20% lower electron density and could possibly result from a well-ordered O or N species, a less well-ordered sulfur species, or compositional heterogeneity. The most interesting development about the detailed geometry of the FeMo-cofactor from the high-resolution refinement is that the Fe-Fe distances between bridged iron sites average ~2.5 Å (range from 2.4 to 2.6 Å), which suggests that there are likely some Fe-Fe bonding interactions that could

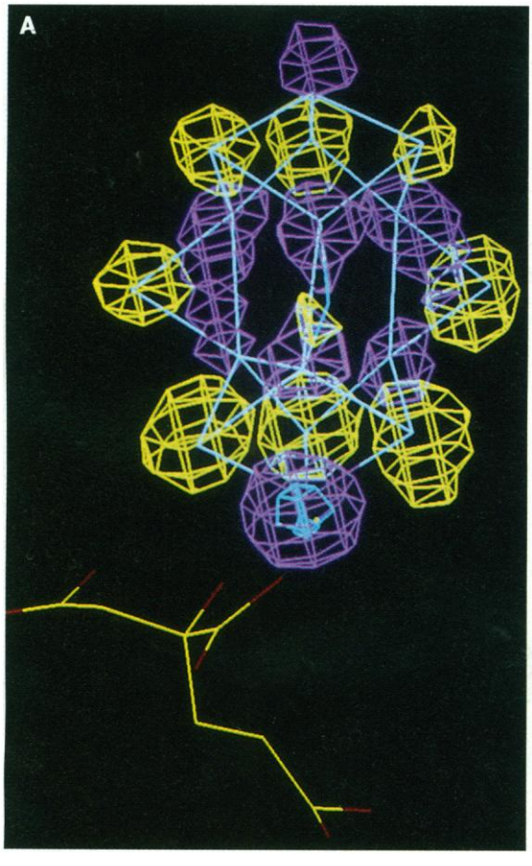


**Fig. 2.** (**A**) $F_o - F_c$ difference map for the FeMo-cofactor at 2.2 Å resolution. Coloring scheme described in legend to Fig. 1, with the addition of a light-blue contour level that is twice that indicated by magenta. The FeMo-cofactor is oriented such that the Y ligand is in front of the cofactor center and the Mo site is at the bottom of the figure. (**B**) Schematic representation of the FeMo-cofactor in the same orientation as (A).

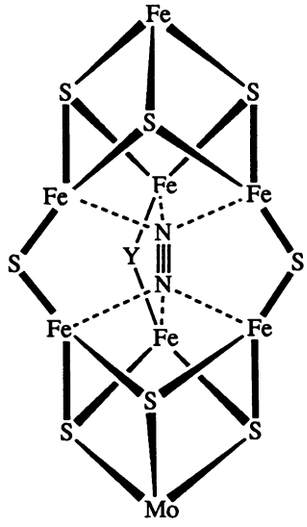


**Fig. 3.** A possible binding mode of $N_2$ in the cavity of the FeMo-cofactor.

provide a fourth coordination interaction for the bridging irons. It is quite clear from these maps that no sulfur is present in the center of the cluster.

Functionally, the details of the interaction between $N_2$ and the FeMo-cofactor are central to the understanding of the catalytic properties of nitrogenase. Although many models can be envisioned for the binding of substrates to the FeMo-cofactor on the basis of the Kim structural model, an intriguing hypothesis can be developed for the coordination mode of $N_2$ to the cofactor that would facilitate triple-bond cleavage. The FeMo-cofactor contains three weak Fe–Fe bonds that are further destabilized by the distortion from idealized tetrahedral geometry. Thus, it is tempting to suggest that $N_2$ could bind in the center of the FeMo-cofactor, thereby replacing the weak Fe–Fe bonds with multiple Fe–N bonds having approximate $sp^3$ geometry (Fig. 3). As a result of these multiple Fe-N interactions, the *sp* hybridized N≡N triple bond should be weakened, thereby lowering the activation barrier for $N_2$ reduction. Features of this model of $N_2$ coordination have been observed for nitrogen analogs binding to trinuclear and dinuclear metal clusters (*11*). Although the cavity size in the FeMo-cofactor structure is too small by ~0.5 Å for $N_2$ to fit in this fashion, the more reduced forms of the cofactor that are believed to actually bind $N_2$ (*12*) may have an increased separation distance between bridged Fe-Fe sites that could accommodate $N_2$ binding. Unlike most substrates and intermediates, however, only $N_2$ is potentially small enough to coordinate inside the FeMo-cofactor, suggesting that alternative binding modes may be utilized by different substrates, reaction intermediates, and inhibitors. This model for the binding of the $N_2$ to the FeMo-cofactor may be useful for the understanding of the mechanistic steps associated with $N_2$ reduction by nitrogenase, and it could guide the development of other hosts and catalysts that can specifically interact with $N_2$.

## REFERENCES AND NOTES


1. B. K. Burgess, in *Advances in Nitrogen Fixation Research*, C. Veeger and W. E. Newton, Eds. (Nijhoff, Boston, 1984), pp. 103–114; .W. H. Orme-Johnson, *Annu. Rev. Biophys. Biophys. Chem.* **14**, 419 (1985); R. H. Holm and E. D. Simhon, in *Molybdenum Enzymes*, T. G. Spiro, Ed. (Wiley, New York, 1985), chap. 2; E. I. Steifel *et al.*, *Am. Chem. Soc. Symp. Ser.* **372**, 372 (1988); R. H. Burris, *J. Biol. Chem.* **266**, 9339 (1991); B. E. Smith and R. R. Eady, *Eur. J. Biochem.* **205**, 1 (1992).
2. J. Kim and D. C. Rees, *Science* **257**, 1677 (1992).
3. W. H. Orme-Johnson, *ibid.*, p. 1639; A. S. Moffat, *ibid.*, p. 1624.
4. CCP4; The SERC (U.K.) Collaborative Computing Project No. 4, A Suite of Programs for Protein Crystallography, distributed from Daresbury Laboratory, Warrington WA4 4AD, United Kingdom.
5. A. T. Brunger, *J. Mol. Biol.* **203**, 803 (1988).
6. D. E. Tronrud, L. F. Ten Eyck, B. W. Matthews, *Acta Crystallogr. Sect. A* **43**, 489 (1987).
7. J. Kim and D. C. Rees, *Nature* **360**, 553 (1992).
8. K. S. Bose, E. Sinn, B. A. Averill, *Organometallics* **3**, 1126 (1984).
9. D. Seyferth, A. M. Kiwan, E. Sinn, *J. Organomet. Chem.* **281**, 111 (1985); H. L. Blonk *et al.*, *Inorg. Chem.* **31**, 962 (1992).
10. M. K. Chan, J. Kim, D. C. Rees, unpublished data.
11. P. E. Baikie and O. S. Mills, *J. Chem. Soc. Chem. Commun.* **1967**, 1228 (1967); C. T.-W. Chu, R. S. Gall, L. F. Dahl, *J. Am. Chem. Soc.* **104**, 737 (1982); D. Sellmann, P. Kreutzer, G. Huttner, A. Frank, *Z. Naturforsch. Teil B* **33**, 1341 (1978); D. Sellmann, W. Soglowek, F. Knoch, M. Moll, *Angew. Chem. Int. Ed. Engl.* **28**, 1271 (1989); G. D. Williams, G. L. Geoffroy, R. R. Whittle, A. L. Rheingold, *J. Am. Chem. Soc.* **107**, 729 (1985); F. A. Cotton, B. E. Hanson, J. D. Jamerson, B. R. Stults, *ibid.* **99**, 3293 (1977); M. D. Brice and B. R. Penfold, *Inorg. Chem.* **11**, 1381 (1972).
12. R. N. F. Thorneley and D. J. Lowe, in *Molybdenum Enzymes*, T. G. Spiro, Ed. (Wiley, New York, 1985), pp. 221–284.


13. Discussions with J. E. Bercaw and J. B. Howard and the assistance of J. Schlessman, T. McPhillips, M. Stowell, A. Chirino, D. Woo, B. T. Hsu, and D. Malerba are appreciated. Research supported by NSF grant DMB 91-18689. M.K.C. is the recipient of NIH fellowship 1F32 GM15006. The rotation camera facility at the Stanford Synchrotron Radiation Laboratory is supported by the Department of Energy, Office of Basic Energy Sciences, and the NIH Biomedical Resource Technology Program, Division of Research Resources. The program X-PLOR was run on the CRAY-YMP at the San Diego Supercomputer Center, supported by NSF.

13 October 1992; accepted 28 January 1993


# The Ischigualasto Tetrapod Assemblage (Late Triassic, Argentina) and $^{40}Ar/^{39}Ar$ Dating of Dinosaur Origins


Raymond R. Rogers, Carl C. Swisher III, Paul C. Sereno, Alfredo M. Monetta, Catherine A. Forster, Ricardo N. Martínez



**$^{40}Ar/^{39}Ar$ dating of sanidine from a bentonite interbedded in the Ischigualasto Formation of northwestern Argentina yielded a plateau age of 227.8 ± 0.3 million years ago. This middle Carnian age is a direct calibration of the Ischigualasto tetrapod assemblage, which includes some of the best known early dinosaurs. This age shifts last appearances of Ischigualasto taxa back into the middle Carnian, diminishing the magnitude of the proposed late Carnian tetrapod extinction event. By 228 million years ago, the major dinosaurian lineages were established, and theropods were already important constituents of the carnivorous tetrapod guild in the Ischigualasto–Villa Unión Basin. Dinosaurs as a whole remained minor components of tetrapod faunas for at least another 10 million years.**


Dinosaurs originated sometime during the Middle to Late Triassic and rose to dominate terrestrial tetrapod communities by the end of the Triassic. The earliest skeletal records of dinosaurs are preserved in Carnian age strata on several continents, including North America (Chinle Group), South America (Ischigualasto and Santa Maria formations), India (Maleri Formation), and Africa (Timesgadiouine Formation) (*1*, *2*). The most complete skeletons of early dinosaurs, discovered in the Ischigualasto Formation of Argentina, include the primitive theropods *Herrerasaurus* and *Eoraptor* (*3*) and the primitive ornithischian *Pisanosaurus* (*4*). These genera, along with *Staurikosaurus* from the Santa Maria Formation of Brazil, have long been considered the oldest dinosaurs (*5*, *6*). Recently, all of these early dinosaur localities were assigned a late Carnian (Tuvalian) age on the basis of biostratigraphic correlations, which suggests that dinosaurs appeared nearly simultaneously across most of Pangea (*7*).

In this report, we present radioisotopic age data from the Ischigualasto Formation and describe the stratigraphic ranges and abundances of Ischigualasto dinosaurs relative to other tetrapods in the paleofauna. These data calibrate the first appearance of dinosaurs and permit a more rigorous evaluation of major extinction and origination events during the Late Triassic (*8*, *9*).

The Ischigualasto Formation is part of the Agua de la Peña Group, a succession of nonmarine Triassic rocks exposed in the Ischigualasto–Villa Unión Basin of northwestern Argentina (Fig. 1). This basin is one of several small rift basins that formed along the western margin of South America before the breakup of Pangea (*10*). The Ischigualasto Formation is composed of fluvial sandstone bodies and fine-grained overbank facies. Deposition occurred on an upland alluvial plain characterized by low sinuosity, shallow streams, occasional lakes, and a seasonal climate (*11*).


R. R. Rogers, Department of Geophysical Sciences, University of Chicago, Chicago, IL 60637.
C. C. Swisher III, Geochronology Center, Institute of Human Origins, Berkeley, CA 94709.
P. C. Sereno and C. A. Forster, Department of Organismal Biology and Anatomy, University of Chicago, Chicago, IL 60637.
A. M. Monetta and R. N. Martínez, Museo de Ciencias Naturales, Universidad Nacional de San Juan, San Juan 5400, Argentina.